Geophysical Research Letters

RESEARCH LETTER
10.1029/2018GL079566

Proxy-Based Assessment of Strength and Frequency of Meteotsunamis in Future Climate

Ivica Vilibić[1], Jadranka Šepić[1], Natalija Dunić[1], Florence Sevault[2], Sebastian Monserrat[3], and Gabriel Jordà[3,4]

[1]Institute of Oceanography and Fisheries, Split, Croatia, [2]CNRM UMR 3589, Météo-France, Toulouse, France, [3]Department of Physics, University of the Balearic Islands, Palma de Mallorca, Spain, [4]Instituto Español de Oceanografía, Centre Oceanogràfic de Balears, Palma de Mallorca, Spain

Abstract A climate synoptic meteotsunami index has been constructed using synoptic variables for the Balearic Islands. The index allows for the very first assessment of atmospherically driven intense sea level oscillations at the tsunami timescale (<2 hr) in future climates. The index has been computed using outputs from evaluation, historical, and three scenario MED-11_CNRM Med-CORDEX regional atmospheric climate runs. The reliability of the index has been verified against reanalysis simulations and on documented meteotsunami events. No significant changes in the index are projected under RCP2.6 and RCP4.5 scenarios, while the yearly number of days with meteotsunamis is expected to increase by 34% under the RCP8.5 scenario by the year 2100. This increase will dominantly occur during the summer season (May–August), being contemporaneous with maximum index values. The presented results are relevant for assessment of sea level extremes worldwide, since high-frequency sea level oscillations may contribute up to 40% of the total range.

Plain Language Summary The study aims to develop the proxy methodology to be used for assessment of meteotsunamis—atmospherically driven waves in a tsunami frequency band—in the future climate, as the present climate models are far from reproduction of processes on a minute and a kilometer scale. The proxy estimates are based on connecting synoptic parameters and patterns to the high-frequency sea level observations. The methodology is successfully verified for Ciutadella harbor, a known hot spot for meteotsunamis, on state-of-the-art reanalysis data. It seems that meteotsunamis are likely not to increase in all but business-as-usual (RCP8.5) climate scenarios, where the increase is matching the season when meteotsunami reach their maximum (spring–summer). The methodology might be useful for assessing meteotsunami hazard in future climates, while being applied at places where meteotsunamis are driven dominantly by a single atmospheric process. Global and regional analyses indicate that these might encompass the majority of midlatitudal regions.

Ivica Vilibić and Jadranka Šepić contributed equally to this work.

Key Points:
- A proxy-based index has been developed for assessing meteotsunamigenic potential in future climate
- No significant changes in the index have been found for the RCP2.6 and RCP4.5 scenarios
- The number of days with meteotsunamis is expected to increase by 34% by the end of the century for the RCP8.5 scenario

Correspondence to:
I. Vilibić,
vilibic@izor.hr

Citation:
Vilibić, I., Šepić, J., Dunić, N., Sevault, F., Monserrat, S., & Jordà, G. (2018). Proxy-based assessment of strength and frequency of meteotsunamis in future climate. *Geophysical Research Letters*, *45*. https://doi.org/10.1029/2018GL079566

Received 10 JUL 2018
Accepted 6 SEP 2018
Accepted article online 11 SEP 2018

1. Introduction

It has been found recently that meteotsunamis—atmospherically generated intense long ocean waves in the tsunami frequency band (Bechle et al., 2016; Monserrat et al., 2006; Pattiaratchi & Wijeratne, 2015; Rabinovich & Monserrat, 1996)—and, more generally, high-frequency sea level oscillations (with periods <2 hr) constitute a substantial fragment of the sea level variance and the oscillation range (Tsimplis et al., 2009; Vilibić & Šepić, 2017). This is particularly pronounced in midlatitude low-tidal seas, such as the Mediterranean, where average coastal sea level oscillations at periods below 2 hr are responsible for 40% of the total sea level range (Vilibić & Šepić, 2017). This estimation is based solely on high-resolution (1-min) measurements. To estimate equivalent future climate statistics, one should either model the processes or use a proxy-based assessment.

The first option is currently unaffordable. To model the evolution of high-frequency sea level oscillations, the evolution of their generative force has to be modeled first. High-frequency sea level oscillations are commonly generated by mesoscale atmospheric processes, in particular by atmospheric gravity waves, that is, by associated surface air pressure oscillations characterized by pressure changes of more than 1 hPa over several minutes (Monserrat et al., 1991; Monserrat & Thorpe, 1996; Pellikka et al., 2014). When such intense atmospheric oscillations propagate over the open sea with a speed that is close to

the speed of long ocean waves, atmospheric energy can be efficiently transferred to the ocean through a *Proudman resonance* mechanism (Proudman, 1929). Long ocean waves, which are then formed, can be further amplified by topography on their way to the shore potentially reaching heights of up to several meters by the time they hit the coast (Monserrat et al., 2006; Pattiaratchi & Wijeratne, 2015). Initialization and evolution of the involved atmospheric processes is complex, and these processes are on a small horizontal (O(10 km)) scale, hinting that their reproduction is difficult, even with the state-of-the-art mesoscale atmospheric models (~1-km resolution; Belušić et al., 2007; Horvath & Vilibić, 2014). Climate models, which at best reach a horizontal resolution of ~10 km (Ruti et al., 2016), are thus ineffective in reproducing atmospheric processes governing high-frequency sea level oscillations. We therefore need to use some reliable proxy for assessing evolution of these high-frequency sea level oscillations.

A common characteristic of high-frequency sea level oscillations worldwide is that they dominantly appear in the presence of specific synoptic patterns (Garcies et al., 1996; Šepić, Vilibić, Lafon et al., 2015; Tanaka, 2010; Vilibić & Šepić, 2017). Over the Mediterranean, this pattern is characterized by (i) the stable lower troposphere maintained by a dry and warm air mass moving from the subtropical African regions toward the north and overtopped by (ii) a strong midtroposphere jet embedded within a humid air mass of lowered stability (Šepić, Vilibić, Rabinovich et al., 2015). This pattern provides a background over which atmospheric gravity waves develop and evolve, as it fosters their generation and has long-range spatial extent, the former by providing areas of instability and the latter being favorable to the presence of a *wave duct* mechanism (Lindzen & Tung, 1976). Due to its large scale (O(100–1,000 km), this synoptic pattern is reproducible by climate models.

A relationship between synoptic patterns and high-frequency sea level oscillations has been recently quantified for Ciutadella, a known meteotsunami hot spot in the Balearic Islands, Western Mediterranean (Šepić et al., 2016). This was done by constructing a meteotsunami index, that is, a variable that links the wave height of measured high-frequency sea level oscillations to a linear combination of synoptic variables. From that study, it can be inferred that (i) the meteotsunami index is highly correlated to high-frequency sea level oscillations; (ii) if the index has a value lower than its 90th percentile, even a weak to moderate meteotsunami (120 cm $>$ wave height $>$ 60 cm) is unlikely to occur; (iii) if the index has a value higher than its 97.5th percentile, there is an ~15% chance that a strong meteotsunami (wave height $>$ 120 cm) will happen; (iv) there are, on average, ~9 days/year where strong tsunamigenic synoptic conditions exist in the present climate (1979–2015), of which ~1.3 days experience meteotsunamis with wave heights surpassing 120 cm. These conclusions are a derivative of the presented results to follow the percentile statistics and thresholds used in this paper, while Šepić et al. (2016) used prescribed index values as thresholds.

The quoted study further suggested that a meteotsunami index might be used as a tool to assess meteotsunami occurrence rates of past, present, and future climates. In this paper, we focus on the creation and verification of a climate meteotsunami index for the area of the Balearic Islands, upon which evolution of the index during the 21st century is assessed under different future scenarios of greenhouse gas (GHG) emissions.

2. Construction and Validation of the Index

Šepić et al. (2016) constructed a synoptic meteotsunami index by correlating a linear combination of atmospheric variables from the ERA-Interim reanalysis with high-frequency sea level oscillations measured at the meteotsunami hot spot in Ciutadella. Here, following the same methodology, we construct a corresponding index using the outputs from the MED-11_CNRM-CM5 regional climate model, based on the mesoscale atmospheric model Aladin version 5.2, which has been found to reproduce synoptics at the level of the ERA-Interim reanalysis (Belušić et al., 2017). Model details are available in Colin et al. (2010) and Panthou et al. (2016). In this study, we use the outputs from five simulations: the *evaluation* run (EVAL), in which the regional model is nested into the ERA-Interim for the period 1979–2012; the *historical* run (HIST), in which the model is nested into the Centre National de Recherches Météorologiques global model constrained only by observed GHG emissions for the period 1950–2005; and three *scenario* runs, in which the same modeling system is run for the period 2006–2100 under different scenarios of GHG emissions: an optimistic one (RCP2.6) in which GHG emissions are reduced substantially over time, resulting in

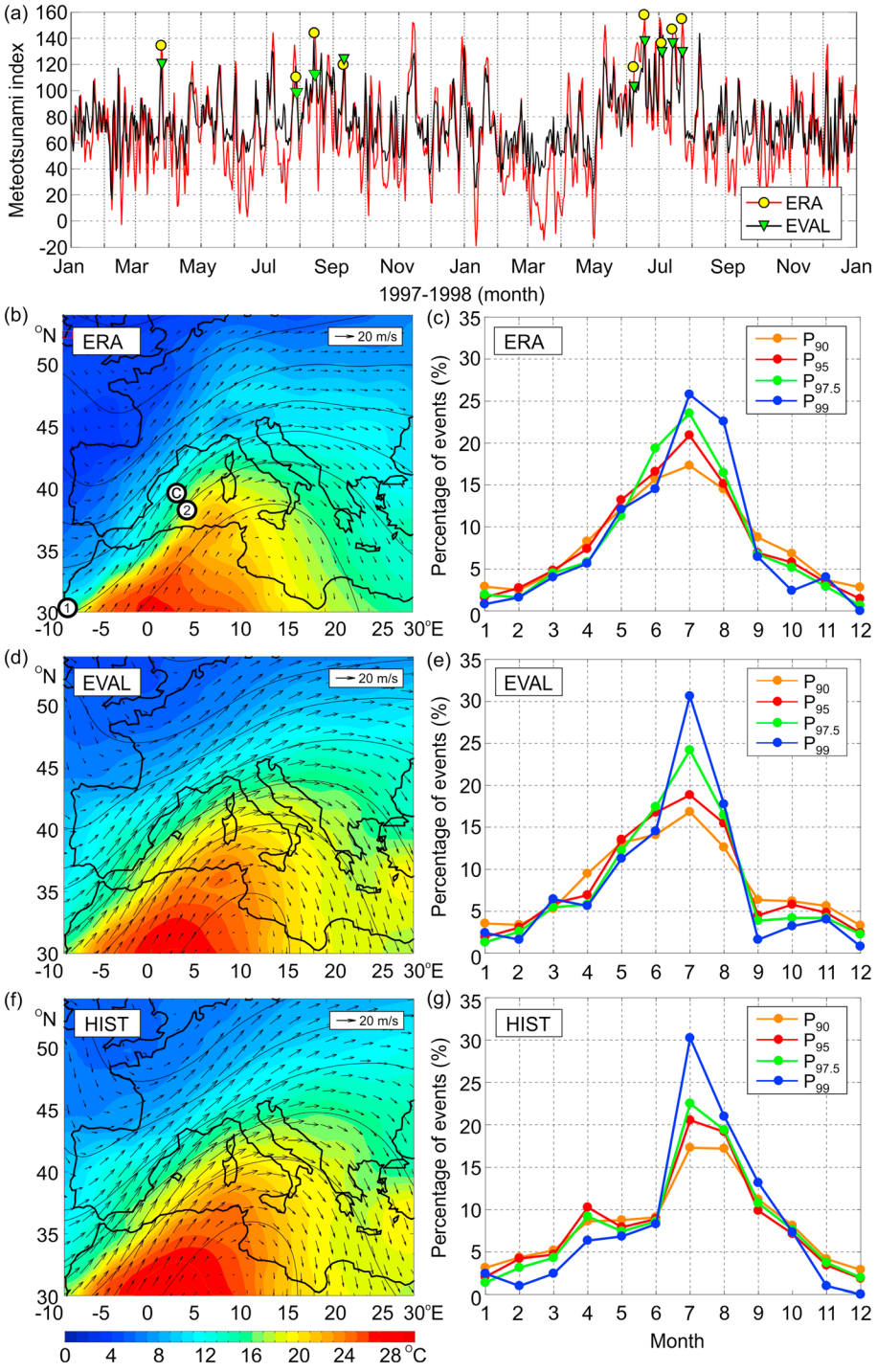

Figure 1. (a) Time series of ERA and EVAL climate meteotsunami indices μ during 1997 and 1998, values of indices during recorded meteotsunami events are marked with yellow circles (ERA) and green triangles (EVAL); (b), (d), and (f) 500-hPa winds and 850-hPa temperature averaged for 20 synoptic situations with the largest values of μ of ERA, EVAL, and HIST run, respectively; (c), (e), and (g) seasonal distribution of percentage of μ above different percentiles (the 90th, 95th, 97.5th, and 99th percentile) for ERA, EVAL, and HIST run, respectively. The geographical locations of points C, 1, and 2 used for construction of μ are indicated in (b). EVAL = evaluation run; HIST = historical run.

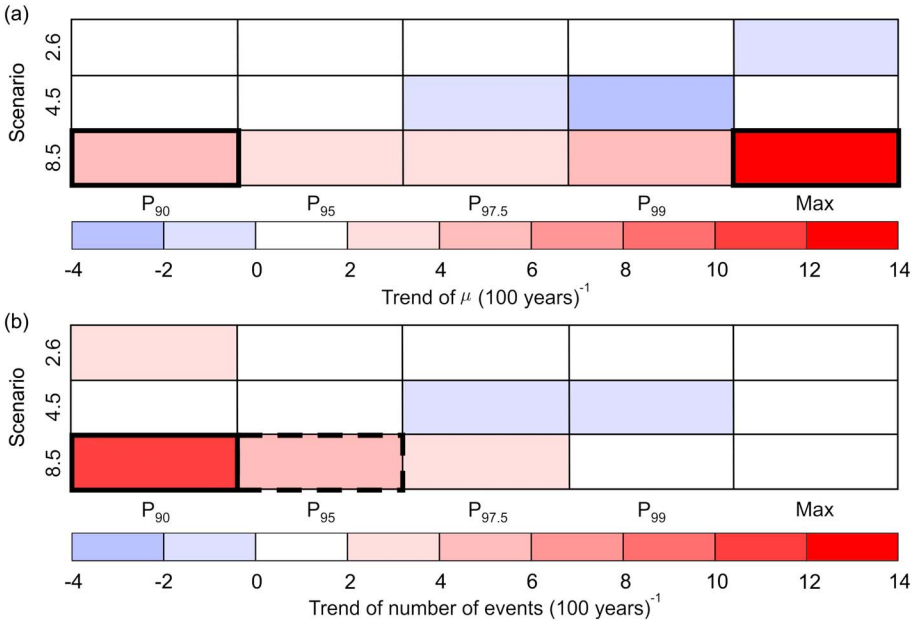

Figure 2. Trends in (a) yearly percentiles of μ established in each RCP run (RCP2.6, RCP4.5, and RCP8.5) and (b) number of yearly events in each RCP run for which μ exceeds the percentile threshold established in the HIST run. Trends that are significant at the 0.05 and 0.10 levels are bounded with thick and dashed lines, respectively. HIST = historical run.

a decrease in total radiative forcing by 2100; a moderate one (RCP4.5) in which total radiative forcing is stabilized before 2100; and a typical scenario (RCP8.5) in which GHG emissions, and resulting total radiative forcing, are increased over time (IPCC, 2014). All model data are available on the Med-CORDEX database (www.medcordex.eu).

The climate meteotsunami index μ is constructed, following methodology by Šepić et al. (2016) from five climate variables x_i:

$$\mu = \sum_{i=1}^{5} A_i x_i, \tag{1}$$

where A_i are linear coefficients obtained by the least-squares method, that is, by fitting synoptic variables originating from the EVAL run to the meteotsunami index based on ERA-Interim variables. We have used the ERA-Interim-based index as the reference because it was not possible to directly fit EVAL synoptic variables to sea level measurements, due to the mismatch of data availability: the EVAL run spans the period from 1979 to 2012 and has an available 1-min continuous sea level series start in 2013. The following variables were used to construct meteotsunami indices: (i = 1) vertical difference between the 48° (directed toward the entrance to Ciutadella) component of winds at 500 hPa and surface winds over Ciutadella at point C (Figure 1), (i = 2) horizontal mean sea level pressure difference between points C and 1, (i = 3) vertical temperature difference between 850 and 925 hPa over Ciutadella at point C, (i = 4) relative humidity at 500 hPa over Ciutadella at point C, and (i = 5) horizontal geopotential difference between points C and 2 at 500 hPa. Coefficients A_i are later used to estimate μ for the historical and scenario runs. This represents a slightly different set of variables than the one used by Šepić et al. (2016). In the original analysis, variables (i = 1) and (i = 5) were taken from the 550 hPa height, with the variable (i = 1) constructed as a vertical difference of absolute values of wind speeds. The former change is due to unavailability of 550-hPa fields in Med-CORDEX database, and the latter was necessary in order to ensure that the climate index properly recognizes and extracts meteotsunamigenic conditions. The original ERA index was reconstructed using a new set of variables; all its properties were kept, with a high correlation in measured sea level heights.

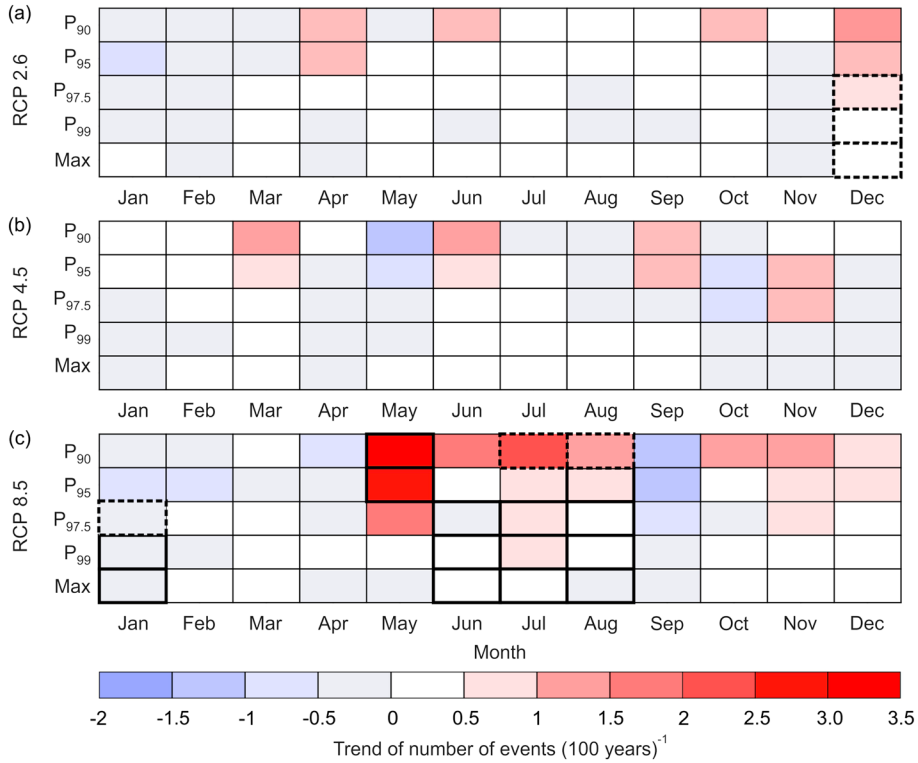

Figure 3. RCP2.6, RCP4.5, and RCP8.5 scenario monthly trends of the number of events for which μ was above a given threshold (the 90th, 95th, 97.5th, and 99th percentile, the maximum) estimated from the historical run. Trends that are significant at the 0.05 and 0.10 levels are bounded with thick and dashed lines, respectively.

A comparison of μ estimated from ERA, EVAL, and HIST runs is provided in Figure 1. The time series of μ obtained from ERA and EVAL runs show good agreement (Figure 1a, $r = 0.81$, $p < 0.001$). For 27 meteotsunami events measured and/or observed at Ciutadella between 1981 and 2006 (Šepić et al., 2009), ERA (EVAL) indices are always above the 79th (88th) percentile for events with wave heights <120 cm and mostly above the 95th percentile for strong events with wave heights >120 cm. Only one out of nine known strong events is associated with a low ERA (EVAL) index ranked as 92 (91) percentile. Average percentile value of ERA (EVAL) index during strong meteotsunamis is 97.6 (97.3).

Spatial patterns averaged over 20 situations during which μ was largest in ERA, over 20 situations during which μ was largest in EVAL, and over 20 situations during which μ was largest in HIST are shown in Figure 1. It should be emphasized that the chronology in extreme events between EVAL and HIST is not preserved, as EVAL contains realistic climatology while HIST is a climate model forced by GHG only. Both EVAL and HIST runs extract meteotsunamigenic conditions properly (compare Figures 1d and 1f with Figure 1b): the strong SW midtroposphere jet overtops the inflow of warm and dry air in the lower troposphere, with strong SE-NW 850-hPa temperature gradients, all found conducive for generation of long-range spatial extent of tsunamigenic air pressure disturbances (Jansà et al., 2007; Šepić, Vilibić, Rabinovich, et al., 2015). Finally, the seasonal distribution of percentiles of meteotsunamigenic conditions is in line with known seasonal distribution of meteotsunamis (Figures 1c, 1e, and 1g), which have a maximum occurrence rate in summer months (Garcies et al., 1996; Monserrat et al., 1991). The seasonality is more pronounced for higher percentiles, that is, for extreme events.

3. The Index in the Future Climate

Trends in μ percentile values are weak and insignificant for all yearly percentiles for the RCP2.6 and RCP4.5 scenarios (Figure 2a). However, the trends become significantly positive (at 95%) for the RCP8.5 scenario run, for the 90th percentile and yearly maximum values. For the 95th to 99th percentiles, the trend in μ is

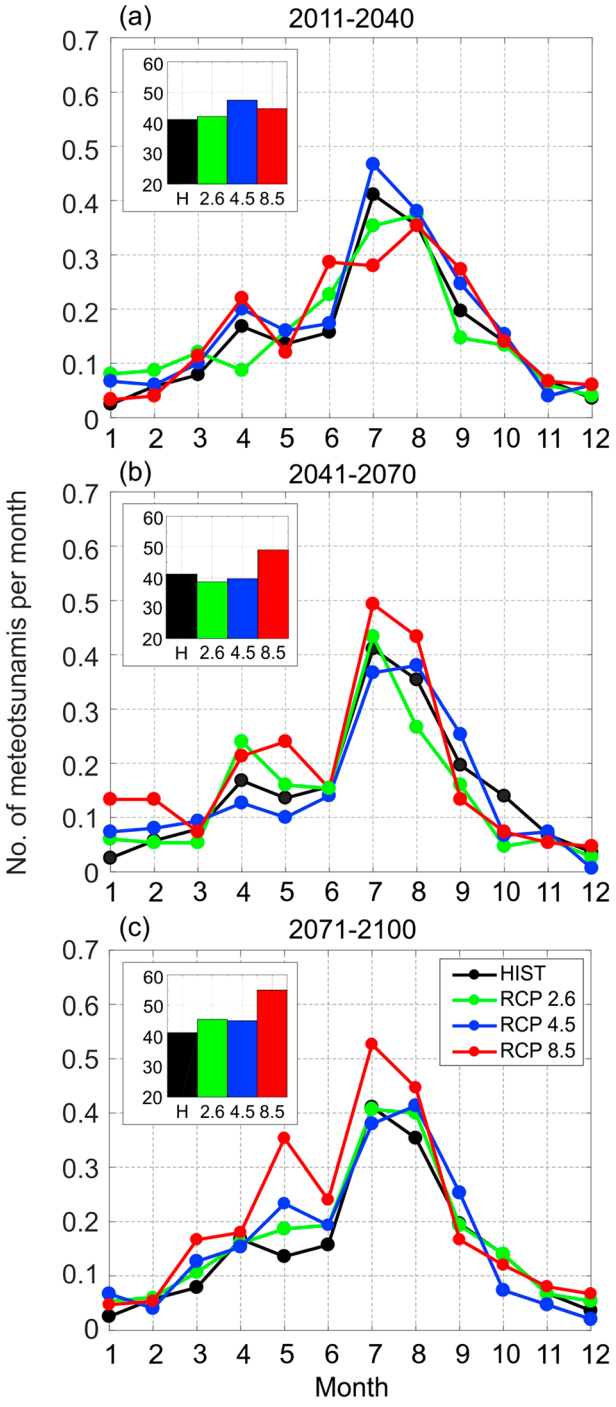

Figure 4. Projected number of meteotsunami events per month and scenarios in three climate periods: (a) 2011–2040, (b) 2041–2070, and (c) 2071–2100. The total number of meteotsunami events per period is shown in the insets. Strong meteotsunami events are defined to occur in 15% of occasions for which μ is higher than the 97.5th percentile of HIST μ; following the methodology by Šepić et al. (2016). HIST = historical run.

positive but not statistically significant due to higher variability in year-to-year changes in higher percentiles of μ. Looking at the number of days for which μ for the Representative Concentration Pathways (RCP) scenarios is higher than a threshold percentile of μ for the HIST run (Figure 2b), the trends are weak and insignificant for the RCP2.6 and RCP4.5 scenarios but positive and significant for the 90th and 95th percentiles for the RCP8.5 scenario. This implies an increase in the number of days with tsunamigenic synoptic conditions ($\mu >$ 95th percentile of HIST run) of >4 days/year at the end of the century.

Analysis conducted on a monthly scale reveals a significant increase in the number of days with the tsunamigenic synoptic conditions during summer, but only for RCP8.5 scenario (Figure 3). This increase is more evident between May and August, that is, during the period within which synoptic conditions favorable for meteotsunamis are most common (Figure 1). The increase in spring (May) particularly refers to the lower percentiles, for example, the number of days in a month with tsunamigenic synoptic conditions exceeding the 90th (95th) percentile in the HIST run, and will increase to more than 3 (2.5) in May. The increase during June to August is, however, projected to be significant for higher percentiles (>97.5th and maximum), that is, precisely for index values which lead to the strongest meteotsunamis. For RCP2.6 and RCP4.5, no significant changes (at 95%) in tsunamigenic synoptic conditions are found for any month.

When looking at the number of meteotsunami events, defined following Šepić et al. (2016) as 15% of the days in which μ is above the 97.5th percentile of HIST μ, the shape of their seasonal distribution does not change substantially between different future periods (Figure 4). Regarding the present climate (black line in plots), the maximum number of events in HIST occurs in July–August, and an approximately two times smaller secondary maximum is distinguishable in April, while meteotsunamis are rare between November and March. Despite a general similarity in seasonal distributions, considerable differences in the expected number of meteotsunami days are found between future climate periods: (i) the number of days with meteotsunamis in July to August increases from approximately 0.35 in 2011–2040 to 0.52 in 2071–2100 in RCP8.5; (ii) a secondary maximum in April is present during 2011–2040; and in RCP8.5, it shifts to May during 2041–2070 and 2071–2100, increasing by approximately 50% during the latter period; (iii) the RCP2.6 distribution shows no spring maximum in 2011–2040 and 2071–2100 and an April to May maximum in 2041–2070; (iv) the least change in number of expected days with meteotsunamis may be found in the wintertime, between September and March; and (v) the total number of expected days with meteotsunamis is constantly increasing with time in the RCP8.5 scenario.

The most important finding originating from our analysis is that total number of expected days with meteotsunamis in the RCP8.5 scenario is projected to consistently increase with time. It has been found to be larger by 9%, 19%, and 34% than in the HIST run in 2011–2040, 2041–2070, and 2071–2100, respectively, with the last change significant at the $p < 0.05$ level. The 2071–2100 period versus HIST period increase in the total number of days is far lower for the RCP2.6 and RCP4.5 scenarios but not larger than 11% and not found to be significant.

4. Discussion and Conclusions

The following conclusions may be drawn from the results presented in this study, which focused on an assessment of tsunamigenic synoptic conditions in the future climate at Ciutadella, a meteotsunami hot spot in the Mediterranean Sea:

1. Synoptic meteotsunami indices have been constructed and proven reliable (Figure 1), allowing for the very first estimation of future climate synoptic meteotsunami indices from RCP climate simulations and therefore initial assessment of meteotsunamis in future climates.
2. No significant changes in tsunamigenic synoptic conditions have been projected for the RCP2.6 and RCP4.5 climate scenarios (Figures 2–4).
3. A significant increase of approximately 34% in the number of days where synoptic conditions are favorable for strong meteotsunamis is foreseen for a business-as-usual climate scenario of GHG emissions (RCP8.5) by the end of the 21st century (Figure 4c). This significant increase is projected for the summer months, when meteotsunamis commonly occur (Figure 3c). This increase might be associated with the increased meridional variability and poleward displacement of the subtropical jet stream (Hudson, 2012), thus increasing the days with southeastern flow over the Western Mediterranean. The impact by El Niño to the European climate might also have an effect on the subtropical jet stream, foreseen to be the largest in typical climate scenarios (Herceg Bulić et al., 2012).

High-frequency sea level oscillations ($<$2 hr) have not been considered in any study of sea level extremes of present and future climates, although their contribution to sea level extremes is considerable, and they are occasionally responsible for extensive damage and even human losses (e.g., Hibiya & Kajiura, 1982; Okal et al., 2014; Pattiaratchi & Wijeratne, 2015; Salaree et al., 2018; Vučetić et al., 2009). In line with that, there are several issues that need to be assessed in future research:

1. As climate models are quite far from reproducing mesoscale atmospheric processes that are generating meteotsunamis, in terms of both their resolution and the imposed physics, a proxy-based approach such as connecting meteotsunamis with tsunamigenic synoptic conditions could be the only way to assess meteotsunami potential in future climates. In this sense, the approach followed here can be applied to any location in the world where high-frequency sea level observations are available to fit the regression model. This presumably encompasses most of the subtropics and midlatitudes, where high correlation exists between winds at 500 mb and high-frequency sea level oscillations (Vilibić & Šepić, 2017). Moreover, as sea level oscillations at the tsunami timescale (between a minute and a few hours) are found to be quite important for sea level extremes (Tsimplis et al., 2009; Vilibić & Šepić, 2017), the presented tool might allow for a better assessment of the forcing mechanisms behind sea level extremes for both present climate and future climate scenarios.
2. Our results for Ciutadella harbor are based on the outputs of a single regional climate model, so we could not quantify all the sources of uncertainty. A complete uncertainty analysis would require the use of an ensemble of climate simulations. However, this is challenging, as not all variables are commonly stored at subdaily resolution (6 or 12 hr) in databases such as Med-CORDEX or CMIP5.
3. This presented approach might be useful for assessing future climate impacts to coasts and coastal infrastructures, particularly as meteotsunamis are normally adjoined with not only moderate flooding but also with strong currents, which can be very destructive, causing millions of Euros of damage during strong meteotsunamis (Jansà et al., 2007; Thomson et al., 2009; Vilibić et al., 2004; Vučetić et al., 2009).

Acknowledgments
We sincerely thank Centre National de Recherches Météorologiques for providing access to variables sourced from EVAL, HIST, RCP2.6, RCP4.5, and RCP8.5 simulations, Ports de les Illes Balears, Govern de les Illes Balears, Palma de Mallorca for providing us with tide gauge data at Ciutadella, and the European Centre for Medium-Range Weather Forecasts for providing the atmospheric reanalysis data (accessible at www.ecmwf.int). Comments raised by two anonymous reviewers were greatly appreciated. S.M. and G.J. acknowledge the support of the CLIFISH project (Spanish MINECO grant CTM2015-66400-C3-2-R).The study has been supported by projects MESSI (UKF grant 25/15) and ADIOS (Croatian Science Foundation grant IP-2016-06-1955).

References

Bechle, A. J., Wu, C. H., Kristovich, D. A. R., Anderson, E. J., Schwab, D. J., & Rabinovich, A. B. (2016). Meteotsunamis in the Laurentian Great Lakes. *Scientific Reports*, *6*(1), 37832. https://doi.org/10.1038/srep37832

Belušić, A., Telišman Prtenjak, M., Güttler, I., Ban, N., Leutwyler, D., & Schär, C. (2017). Near-surface wind variability over the broader Adriatic region: Insights from an ensemble of regional climate models. *Climate Dynamics*, *50*(11–12), 4455–4480. https://doi.org/10.1007/s00382-017-3885-5

Belušić, D., Grisogono, B., & Bencetić Klaić, Z. (2007). Atmospheric origin of the devastating coupled air-sea event in the east Adriatic. *Journal of Geophysical Research*, *112*, D17111. https://doi.org/10.1029/2006JD008204

Colin, J. M., Déqué, M., Radu, R., & Somot, S. (2010). Sensitivity study of heavy precipitations in limited area model climate simulation: Influence of the size of the domain and the use of the spectral nudging technique. *Tellus A*, *62*(5), 591–604. https://doi.org/10.1111/j.1600-0870.2010.00467.x

Garcies, M., Gomis, D., & Monserrat, S. (1996). Pressure-forced seiches of large amplitude in inlets of the Balearic Islands. Part II: Observational study. *Journal of Geophysical Research*, *101*(C3), 6453–6467. https://doi.org/10.1029/95JC03626

Herceg Bulić, I., Branković, Č., & Kucharski, F. (2012). Winter ENSO teleconnections in a warmer climate. *Climate Dynamics*, *38*(7-8), 1593–1613. https://doi.org/10.1007/s00382-010-0987-8

Hibiya, T., & Kajiura, K. (1982). Origin of 'Abiki' phenomenon (kind of seiches) in Nagasaki Bay. *Journal of the Oceanographic Society of Japan*, *38*(3), 172–182. https://doi.org/10.1007/BF02110288

Horvath, K., & Vilibić, I. (2014). Atmospheric mesoscale conditions during the Boothbay meteotsunami: A numerical sensitivity study using a high-resolution mesoscale model. *Natural Hazards*, *74*(1), 55–74. https://doi.org/10.1007/s11069-014-1055-1

Hudson, R. D. (2012). Measurements of the movement of the jet streams at mid-latitudes, in the Northern and Southern Hemispheres, 1979 to 2010. *Atmospheric Chemistry and Physics*, *12*, 7797–7808.

IPCC (2014). *Climate change 2014: Synthesis report. Contribution of Working Groups I, II and III to the Fifth Assessment Report of the Intergovernmental Panel on Climate Change* [Core Writing Team, R.K. Pachauri and L.A. Meyer (eds.)]. IPCC, Geneva, Switzerland, 151 pp.

Jansà, A., Monserrat, S., & Gomis, D. (2007). The rissaga of 15 June 2006 in Ciutadella (Menorca), a meteorological tsunami. *Advances in Geosciences*, *12*, 1–4. https://doi.org/10.5194/adgeo-12-1-2007

Lindzen, R. S., & Tung, K.-K. (1976). Banded convective activity and ducted gravity waves. *Monthly Weather Review*, *104*(12), 1602–1617. https://doi.org/10.1175/1520-0493(1976)104<1602:BCAADG>2.0.CO;2

Monserrat, S., Rabinovich, A. B., & Vilibić, I. (2006). Meteotsunamis: Atmospherically induced destructive ocean waves in the tsunami frequency band. *Natural Hazards and Earth System Sciences*, *6*(6), 1035–1051. https://doi.org/10.5194/nhess-6-1035-2006

Monserrat, S., Ramis, C., & Thorpe, A. J. (1991). Large-amplitude pressure oscillations in the Western Mediterranean. *Geophysical Research Letters*, *18*(2), 183–186. https://doi.org/10.1029/91GL00234

Monserrat, S., & Thorpe, A. J. (1996). Use of ducting theory in an observed case of gravity waves. *Journal of the Atmospheric Sciences*, *53*(12), 1724–1736. https://doi.org/10.1175/1520-0469(1996)053<1724:UODTIA>2.0.CO;2

Okal, E. A., Visser, J. N., & de Beer, C. H. (2014). The Dwarskersbos, South Africa local tsunami of August 27, 1969: Field survey and simulation as a meteorological event. *Natural Hazards*, *74*(1), 251–268. https://doi.org/10.1007/s11069-014-1205-5

Panthou, G., Vrac, M., Drobinski, P., Bastin, S., & Li, L. (2016). Impact of model resolution and Mediterranean Sea coupling on hydrometeorological extremes in RCMs in the frame of HyMeX and MED-CORDEX. *Climate Dynamics*, *51*(3), 915–932. https://doi.org/10.1007/s00382-016-3374-2

Pattiaratchi, C. B., & Wijeratne, E. M. S. (2015). Are meteotsunamis an underrated hazard? *Philosophical Transactions of the Royal Society A*, *373*(2053), 20140377. https://doi.org/10.1098/rsta.2014.0377

Pellikka, H., Rauhala, J., Kahma, K. K., Stipa, T., Boman, H., & Kangas, A. (2014). Recent observations of meteotsunamis on the Finnish coast. *Natural Hazards*, *74*(1), 197–215. https://doi.org/10.1007/s11069-014-1150-3

Proudman, J. (1929). The effects on the sea of changes in atmospheric pressure. *Geophysical Supplements to the Monthly Notices of the Royal Astronomical Society*, *2*(4), 197–209. https://doi.org/10.1111/j.1365-246X.1929.tb05408.x

Rabinovich, A. B., & Monserrat, S. (1996). Meteorological tsunamis near the Balearic and Kuril Islands: Descriptive and statistical analysis. *Natural Hazards*, *13*(1), 55–90. https://doi.org/10.1007/BF00156506

Ruti, P., Somot, S., Giorgi, F., Dubois, C., Flaounas, E., Obermann, A., et al. (2016). Med-CORDEX initiative for Mediterranean climate studies. *Bulletin of the American Meteorological Society*, *97*(7), 1187–1208. https://doi.org/10.1175/BAMS-D-14-00176.1

Salaree, A., Mansouri, R., & Okal, E. A. (2018). The intriguing tsunami of 19 March 2017 at Bandar Dayyer, Iran: Field survey and simulations. *Natural Hazards*, *90*(3), 1277–1307. https://doi.org/10.1007/s11069-017-3119-5

Šepić, J., Vilibić, I., Lafon, A., Macheboeuf, L., & Ivanović, Z. (2015). High-frequency sea level oscillations in the Mediterranean and their connection to synoptic patterns. *Progress in Oceanography*, *137*, 284–298. https://doi.org/10.1016/j.pocean.2015.07.005

Šepić, J., Vilibić, I., & Monserrat, S. (2009). Teleconnections between the Adriatic and the Balearic meteotsunamis. *Physics and Chemistry of the Earth*, *34*, 928–937. https://doi.org/10.1016/j.pce.2009.08.007

Šepić, J., Vilibić, I., & Monserrat, S. (2016). Quantifying the probability of meteotsunami occurrence from synoptic atmospheric patterns. *Geophysical Research Letters*, *43*, 10,377–10,384. https://doi.org/10.1002/2016GL070754

Šepić, J., Vilibić, I., Rabinovich, A. B., & Monserrat, S. (2015). Widespread tsunami-like waves of 23–27 June in the Mediterranean and Black Seas generated by high-altitude atmospheric forcing. *Scientific Reports*, *5*(1), 11682. https://doi.org/10.1038/srep11682

Tanaka, K. (2010). Atmospheric pressure-wave bands around a cold front resulted in a meteotsunami in the East China Sea in February 2009. *Natural Hazards and Earth System Sciences*, *10*(12), 2599–2610. https://doi.org/10.5194/nhess-10-2599-2010

Thomson, R. E., Rabinovich, A. B., Fine, I. V., Sinnott, D. C., McCarthy, A., Sutherland, N. A. S., & et al. (2009). Meteorological tsunamis on the coasts of British Columbia and Washington. *Physics and Chemistry of the Earth*, *34*(17–18), 971–988. https://doi.org/10.1016/j.pce.2009.10.003

Tsimplis, M. N., Marcos, M., Perez, B., Challenor, P., Garcia-Fernandez, M. J., & Raicich, F. (2009). On the effect of the sampling frequency of sea level measurements on return period estimate of extremes—Southern European examples. *Continental Shelf Research*, *29*(18), 2214–2221. https://doi.org/10.1016/j.csr.2009.08.015

Vilibić, I., Domijan, N., Orlić, M., Leder, N., & Pasarić, M. (2004). Resonant coupling of a traveling air-pressure disturbance with the east Adriatic coastal waters. *Journal of Geophysical Research*, *109*, C10001. https://doi.org/10.1029/2004JC002279

Vilibić, I., & Šepić, J. (2017). Global mapping of nonseismic sea level oscillations at tsunami timescales. *Scientific Reports*, *7*(1), 40818. https://doi.org/10.1038/srep40818

Vučetić, T., Vilibić, I., Tinti, S., & Maramai, A. (2009). The Great Adriatic flood of 21 June 1978 revisited: An overview of the reports. *Physics and Chemistry of the Earth*, *34*(17–18), 894–903. https://doi.org/10.1016/j.pce.2009.08.005